

Alteration of Epithelial Structure and Function Associated with PtdIns(4,5)P₂ Degradation by a Bacterial Phosphatase

David Mason,¹ Gustavo V. Mallo,¹ Mauricio R. Terebiznik,¹ Bernard Payraastre,² B. Brett Finlay,³ John H. Brumell,^{1,4} Lucia Rameh,⁵ and Sergio Grinstein¹

¹Cell Biology Program, Hospital for Sick Children and Department of Biochemistry, University of Toronto, Toronto, Ontario, M5G 1X8, Canada

²Inserm U563, Department of Oncogenesis and Signal Transduction in Hematopoietic Cells, Hopital Purpan, Toulouse, France

³Michael Smith Laboratory, University of British Columbia, Vancouver, British Columbia V6T 1Z3, Canada

⁴Department of Medical Genetics and Microbiology, University of Toronto, Ontario, M5G 1X8, Canada

⁵Boston Biomedical Research Institute, Watertown, MA 02472

Elucidation of the role of PtdIns(4,5)P₂ in epithelial function has been hampered by the inability to selectively manipulate the cellular content of this phosphoinositide. Here we report that SigD, a phosphatase derived from *Salmonella*, can effectively hydrolyze PtdIns(4,5)P₂, generating PtdIns(5)P. When expressed by microinjecting cDNA into epithelial cells forming confluent monolayers, wild-type SigD induced striking morphological and functional changes that were not mimicked by a phosphatase-deficient SigD mutant (C462S). Depletion of PtdIns(4,5)P₂ in intact SigD-injected cells was verified by detachment from the membrane of the pleckstrin homology domain of phospholipase C δ , used as a probe for the phosphoinositide by conjugation to green fluorescent protein. Single-cell measurements of cytosolic pH indicated that the Na⁺/H⁺ exchange activity of epithelia was markedly inhibited by depletion of PtdIns(4,5)P₂. Similarly, anion permeability, measured using two different halide-sensitive probes, was depressed in cells expressing SigD. Depletion of PtdIns(4,5)P₂ was associated with marked alterations in the actin cytoskeleton and its association with the plasma membrane. The junctional complexes surrounding the injected cells gradually opened and the PtdIns(4,5)P₂-depleted cells eventually detached from the monolayer, which underwent rapid restitution. Similar observations were made in intestinal and renal epithelial cultures. In addition to its effects on phosphoinositides, SigD has been shown to convert inositol 1,3,4,5,6-pentakisphosphate (IP₅) into inositol 1,4,5,6-tetrakisphosphate (IP₄), and the latter has been postulated to mediate the diarrhea caused by *Salmonella*. However, the effects of SigD on epithelial cells were not mimicked by microinjection of IP₄. In contrast, the cytoskeletal and ion transport effects were replicated by hydrolyzing PtdIns(4,5)P₂ with a membrane-targeted 5-phosphatase or by occluding the inositide using high-avidity tandem PH domain constructs. We therefore suggest that opening of the tight junctions and inhibition of Na⁺/H⁺ exchange caused by PtdIns(4,5)P₂ hydrolysis combine to account, at least in part, for the fluid loss observed during *Salmonella*-induced diarrhea.

INTRODUCTION

Phosphatidylinositol 4,5-bisphosphate (PtdIns(4,5)P₂) has long been recognized as an important source of second messengers. Hydrolysis of PtdIns(4,5)P₂ by phospholipase C yields diacylglycerol, a potent activator of most protein kinase C isoforms and other enzymes bearing C1 domains, and inositol 1,4,5-trisphosphate, which induces release of calcium stored in the endoplasmic reticulum (Taylor, 2002). In addition, phosphorylation of PtdIns(4,5)P₂ by class I phosphatidylinositol 3-kinases generates phosphatidylinositol 3,4,5-trisphosphate, a ligand and activator of various effectors that contain pleckstrin homology (PH) domains (Vanhaesebroeck et al., 2001; Lemmon, 2003). Not only are its metabolites critical for signal transduction, but PtdIns(4,5)P₂ itself serves multiple regulatory functions in the cell.

It affects several stages of actin microfilament assembly and remodeling, including uncapping of barbed ends, severing and bundling of filaments, and de novo nucleation (Hilpela et al., 2004; Roth, 2004). In addition, several studies have shown that a variety of ion channels and exchangers are directly modulated by the local concentration of PtdIns(4,5)P₂ (Leung et al., 2000; Hilgemann et al., 2001; Hilgemann, 2003).

The functional importance of the metabolites generated from PtdIns(4,5)P₂ has been convincingly established by pharmacological means. Potent and reasonably

D. Mason and G.V. Mallo contributed equally to this work.

Correspondence to Sergio Grinstein: sga@sickkids.ca

The online version of this article contains supplemental material.

Abbreviations used in this paper: DAPI, 4',6-diamidino-2-phenyl-indole; DMEM, Dulbecco's modified Eagle's medium; HPLC, high performance liquid chromatography; HPMI, HEPES-buffered solution RPMI-1640; IP₃, inositol 1,4,5-trisphosphate; IP₄, inositol 1,4,5,6-tetrakisphosphate; IP₅, inositol 1,3,4,5,6-pentakisphosphate; MQAE, N-(ethoxycarbonylmethyl)-6-methoxyquinolinium bromide; NHE, Na⁺/H⁺ exchanger; PH, pleckstrin homology; PtdIns(4,5)P₂, phosphatidylinositol 4,5-bisphosphate; TLC, thin layer chromatography.

specific phospholipase C and protein kinase C inhibitors are available, which have been used to evaluate the physiological role of diacylglycerol, inositol 1,4,5-trisphosphate (IP₃), and their effectors (Botelho et al., 2000; Matsui et al., 2001; Spitaler and Cantrell, 2004). Similarly, class I phosphatidylinositol 3-kinases can be selectively inhibited by wortmannin or LY294002 to assess the effects of phosphatidylinositol 3,4,5-trisphosphate biosynthesis (Vieira et al., 2001; Djordjevic and Driscoll, 2002). By contrast, establishing the function of PtdIns(4,5)P₂ has proven to be considerably more difficult. No specific inhibitors of the kinases that generate this phosphoinositide have been described, and the coexistence of multiple kinase isoforms and splice variants has precluded genetic analysis. Definitive confirmation of the involvement of PtdIns(4,5)P₂ in the regulation of ion channels and transporters stems largely from electrophysiological studies in excised patches or perfused cells, where the cytosolic aspect of the membrane can be accessed directly by solutions containing varying amounts of PtdIns(4,5)P₂ or bacterial lipases (Estacion et al., 2001; Loussouarn et al., 2003; Oliver et al., 2004). The multiple actions of PtdIns(4,5)P₂ in cytoskeletal dynamics have been similarly gleaned primarily from studies of disrupted cells (Nebl et al., 2000; Hsin-Yi et al., 2004).

Remarkably little is known about the role of PtdIns(4,5)P₂ in epithelial structure and function. The barrier and vectorial transport functions of epithelia are eminently dependent on the maintenance of the integrity of individual cells and of their intercellular contacts. This requirement rules out the use of most of the techniques that have been successfully applied to study PtdIns(4,5)P₂ function in other systems. Because molecular or genetic manipulation of the kinases that generate PtdIns(4,5)P₂ is subject to the limitations described above, we considered instead the possibility of modulating the cellular PtdIns(4,5)P₂ content by expression of phosphoinositide-specific phosphatases. Some success has been reported using Inp54p, a yeast inositol polyphosphate 5'-phosphatase (Raucher et al., 2000). In our hands, however, this enzyme, as well as the native forms of the mammalian phosphoinositide phosphatases synaptojanin, SKIP and OCRL, had negligible effects on the PtdIns(4,5)P₂ content of epithelial cells (unpublished data). Failure of the phosphatases to target to the plasmalemma and/or to become activated likely account for these observations.

We reported that SigD/SopB, an injected virulence factor of *Salmonella* species, altered the binding of a PtdIns(4,5)P₂-specific PH domain to the inner leaflet of the plasma membrane in HeLa cells (Terebiznik et al., 2002). We now present evidence that SigD/SopB (referred to hereafter as SigD) functions as a 4'-phosphatase that dephosphorylates PtdIns(4,5)P₂ to form PI(5)P. By cloning this bacterial phosphatase into a mammalian expression vector we were able to introduce it by micro-

injection into intact epithelia, which are notoriously refractory to transfection. This strategy enabled us to analyze the consequences of selective depletion of PtdIns(4,5)P₂ in confluent epithelia. Because *Salmonella* is an enteric pathogen that injects SigD along with several other products into host epithelial cells via a type III secretion system encoded by the *Salmonella* pathogenicity island (SPI)-I (Galan, 1998), we focused our study primarily on IEC-18 cells, a line derived from the rat small intestine (Ma et al., 1992). In this manner, we simultaneously learned about the possible consequences of *Salmonella* infection on intestinal physiology.

MATERIALS AND METHODS

Materials and Solutions

IP₄ was purchased from Matreya Inc. Biochemicals. Rhodamine-phalloidin, 4',6-diamidino-2-phenyl-indole (DAPI), FM4-64, SNARF-5F, *N*-(ethoxycarbonylmethyl)-6-methoxyquinolinium bromide (MQAE), and Alexa 568 microinjection dye were from Molecular Probes. Radiolabeled [³²P]γATP and [³H]-myo-inositol were from MP Biomedicals (formerly ICN Biomedicals). The Na⁺/H⁺ exchanger (NHE) inhibitors HOE694 and S3226 were gifts of Hoechst and Aventis, respectively. FBS, α-modified Earle's medium (MEM), Dulbecco's modified Eagle's medium (DMEM), HEPES-buffered solution RPMI-1640 (HPMI), PBS, and penicillin plus streptomycin were from Wisent. Antibodies to ZO-1 were purchased from Zymed Laboratories. Monoclonal antibodies against active caspase 3 were from BD Biosciences. Cy3-conjugated secondary antibodies were from Jackson ImmunoResearch Laboratories. All other reagents were from Sigma-Aldrich. Microinjection buffer consisted of (in mM) 140 KCl plus 10 HEPES, pH 7.4 at 37°C and was filter sterilized before use. Na⁺-rich solution contained 130 NaCl, 3 KCl, 1 CaCl₂, 1 MgCl₂, 20 HEPES, pH 7.4 at 37°C. In K⁺-rich solution, all NaCl was replaced by KCl, and in Cl⁻-depleted solution NaCl was replaced by NaI or NaNO₃.

Cell Culture

HeLa, IEC-18, and OK cells were obtained from the American Tissue Culture Collection. IEC-18 cells were grown in DMEM supplemented with 5% FBS and 0.1 U/ml bovine pancreatic insulin. HeLa cells were grown in DMEM supplemented with 10% FBS. OK cells were grown in α-MEM supplemented with 10% FBS. All cells were maintained under 5% CO₂ at 37°C. When required, cells were pretreated with 100 μM LY294002 for 30 min and the inhibitor was kept in the medium throughout the experiment.

DNA Constructs

The mammalian expression vectors encoding wild-type SigD and the inactive SigD mutant (C462S) have been described elsewhere (Marcus et al., 2001). The vector pEGFP::PLCδPH encodes the PH domain of PLCδ fused to EGFP (PLCδ-PH-GFP). pGFP::PM encodes the myristoylation/palmitoylation sequence from Lyn fused to GFP (PM-GFP). Both of these were the gift of T. Meyer (Stanford University, Stanford, CA) and their construction has been described before (Teruel et al., 1999). 2FYVE-GFP consists of two tandem FYVE domains from EEA1 conjugated to GFP and has been described previously (Vieira et al. 2001). The 2(PLCδ-PH)-GFP construct was made by combining two tandem PLCδ-PH domains to GFP and was a gift of M. Rebecchi (State University of New York, Sunnysbrook, NY). The phosphatase domain of mammalian synaptojanin 2 fused to a CAAX box modeled after the carboxy terminal sequence of K-Ras (PD-CAAX) was the gift of

TABLE I
Analysis of Phosphoinositide Content after Infection

	Uninfected	<i>Salmonella</i> Wild Type	<i>Salmonella</i> $\Delta sigD$
PtdIns(4,5)P ₂	8.2 ± 0.7%	5.3 ± 0.4%	6.9 ± 0.4%
PtdInsP	5.5 ± 0.7%	7.4 ± 0.9%	3.5 ± 0.2%

Phosphoinositide levels were quantified before (Uninfected) and after infection of HeLa cells with either wild-type or *sigD*-deficient ($\Delta sigD$) *Salmonella*. Lipids were extracted and analyzed by HPLC as detailed in Materials and methods. The amount of the phosphoinositides is given as percent of PtdIns in the same sample. PtdInsP refers to the sum of both PtdIns(4)P and PtdIns(5)P, which are not resolved by the chromatographic system used. Data are means ± SEM of three separate experiments.

M. Symons (The Feinstein Institute for Medical Research, Manhasset, NY). The construction of this construct has been detailed previously (Malecz et al., 2000). The plasmid encoding the anion-sensitive mutant of the yellow fluorescent protein YFP(H148Q) was described in Jayaraman et al. (2000).

Bacterial Culture and Infection Protocol

The source and properties of wild-type and SigD-deficient *Salmonella enterica* serovar Typhimurium, ($\Delta sigD$) SL1344, were described previously (Terebiznik et al., 2002). For complementation analysis, the $\Delta sigD$ mutant of *S. Typhimurium* SL1344 was transformed with plasmid pACYC184 encoding either wild-type or the catalytically inactive C462S mutant of SigD (Marcus et al., 2001). That the level of expression of the wild-type and mutant SigD was similar in the bacterial strains used was verified by immunoblotting, using a polyclonal anti-SigD antibody. Overnight bacterial cultures were diluted 1:30 into Luria-Bertani broth and incubated at 37°C, shaking for 3 h. Bacteria were sedimented at 10,000 *g* for 2 min and then resuspended in HPMI, pH 7.4. 1 ml of bacterial suspension was added to cells that had been plated on 10-cm dishes and preincubated with 1 ml of HPMI at 37°C for 5 min. Infection was performed at 37°C under 5% CO₂. After 10 min, excess bacteria were washed away with PBS and the cells subjected to lipid extraction as detailed below.

Lipid Extraction and Phosphoinositide Analysis

Lipid labeling and extraction were performed essentially as described by Carricaburu et al. (2003). In brief, HeLa cells were labeled with 20 μ Ci/ml [³H]-myoinositol for 24–48 h in inositol-free medium. After labeling, the cells were washed free of excess isotope, infected with the indicated strain of *Salmonella* for 15 min, and immediately lysed in 1 M HCl. Lipids were next extracted in chloroform:methanol (1:1, vol:vol) and deacylated as described (Serunian et al., 1991). Deacylated lipids were separated by anion-exchange high performance liquid chromatography (HPLC), detected by an online Radiomatic detector (Perkin Elmer), and quantified relative to PtdIns using the ProFSA analysis program. Individual peaks in the chromatogram were identified using in vitro-synthesized internal standard lipids.

For analysis of phosphatidylinositol 5-phosphate (PtdIns(5)P) the cells were treated as specified in the text and phospholipids were extracted in acidified chloroform:methanol as in Niebuhr et al. (2002). The lipid extracts were dried under nitrogen and used subsequently for determination of PtdIns(5)P content by the method of Morris et al. (2000). In brief, PtdIns(5)P was converted to PtdIns(4,5)P₂ in vitro by addition of phosphatidylinositol 5-phosphate 4-kinase and ³²P- γ ATP. The products of this reaction were separated by thin layer chromatography (TLC) and the amount of radiolabeled PtdIns(4,5)P₂ quantified. The identity of the labeled product was confirmed to be PtdIns(4,5)P₂ by analyzing the samples using HPLC.

Microinjection Protocol

Cells were grown on 25-mm glass coverslips and used for experiments 2 d after the monolayer had reached confluence. The coverslips were then transferred to a thermostatted Leiden chamber and incubated with HPMI medium supplemented with antibiotic/antimycotic mixture (1:500) for 30 min before microinjection. The microinjection solution contained 50 μ g/ml of the indicated mixture of plasmids, typically a 5 to 1 ratio of SigD to PLC δ -PH-GFP cDNA. Microinjection was performed under phase contrast microscopy using an Eppendorf Transjector 5246 controlled by an Eppendorf 5171 Micromanipulator. Microinjected cells were identified by the expression of the fluorescent protein products. To minimize evaporation during prolonged observation periods the chambers were sealed using a second coverslip secured with a small amount of silicon grease.

Cytosolic pH Determinations

For cytosolic pH determinations IEC-18 cells were microinjected with cDNA encoding YFP, with or without SigD cDNA. Cells were next incubated for 3 h at 37°C under 5% CO₂ to allow expression of the proteins. Alternatively, the cells were loaded with SNARF-5F by loading with 20 μ M of the precursor acetoxymethyl ester for 30 min. The coverslips were then mounted in a thermostatted Leiden holder, bathed in a Na⁺-rich buffer, and placed on the stage of a Leica fluorescence microscope equipped with a PL Fluotar 100 \times /1.30 N.A. oil immersion objective. Sutter filter wheels positioned excitation and emission filters in front of a Hg lamp and the acquisition camera, respectively. For YFP, excitation was at 480 nm and was directed to the cells through a 510-nm dichroic mirror. Emitted fluorescence was selected through a 535BP25-nm filter. For SNARF-5F, excitation was at 550 nm and emission was recorded at 580 and 640 nm. Images were captured with an Orca ER cooled charge-coupled device camera (Hamamatsu). Image acquisition was controlled by the Metafluor software v3.5 (Universal Imaging Corp.). To determine background, an area identical to the region of interest was selected outside the transfected cell and fluorescence was acquired. At the end of the experiment, a calibration curve of fluorescence (ratio) vs. pH was obtained in situ by sequential perfusion with K⁺-rich medium buffered to predetermined pH values (between 6.0 and 7.4) containing 10 μ g/ml nigericin. Calibration curves were constructed by plotting the extracellular pH, assumed to be identical to the cytosolic pH under these conditions, against the corresponding fluorescence.

To determine the relative contribution of specific NHE isoforms, pH determinations were performed in the presence of 1 μ M HOE694 to selectively inhibit NHE1, 20 μ M HOE694, to inhibit both NHE1 and NHE2, or 20 μ M HOE694 plus 5 μ M of S3226, to inhibit the three main plasmalemmal isoforms.

Determinations of Anion Permeability

Anion permeability was estimated by two methods: first, the anion-sensitive variant of YFP(H148Q) was used by a microfluorimetric method similar to that described above for pH determinations. Because YFP derivatives are also inherently sensitive to pH, a second series of experiments was performed using a chloride-sensitive dye, *N*-(ethoxycarbonylmethyl)-6-methoxyquinolinium bromide (MQAE), which was loaded into the epithelial cells by hypotonic stress, following expression of SigD or the PD-CAAX construct. To identify the cells expressing the phosphatase, SigD was cotransfected with PLC δ -PH-GFP. By studying the presence and distribution of this construct we not only identified the transfectants, but ensured that the phosphatase had in fact exerted its effects on PtdIns(4,5)P₂. Control experiments were performed in cells expressing PLC δ -PH-GFP only. After loading hypotonically with MQAE, cells were allowed to recover in isotonic medium for 30 min before measurement of anion permeability.

Calibration was made using 10 μM nigericin and 10 μM tributyltin chloride in K^+ -rich media of varying Cl^- concentration.

Staining with Fluorescent Markers and Confocal Microscopy

Cells grown on coverslips were washed twice with PBS and fixed in 4% paraformaldehyde in PBS at room temperature for at least 30 min, followed by quenching of excess fixative with 100 mM glycine for 10 min. Cells were blocked while permeabilized using 5% skimmed milk in PBS containing 0.1% Triton X-100 for 60 min. ZO-1 was immunostained using a polyclonal primary antibody (1:100), followed by secondary Cy3-conjugated donkey anti-rabbit antibodies (1:1,000).

To label F-actin, fixed and permeabilized cells were stained with a 1:500 dilution of rhodamine-phalloidin for 30 min. Two different methods were used for assessment of apoptosis. In both cases the cells were fixed with 3% paraformaldehyde for 15 min at room temperature and, where indicated, permeabilized with 0.1% saponin in PBS. For caspase-3 staining the preparation was blocked for 30 min in medium containing 10% donkey serum in PBS, and then incubated with antibody to active caspase-3 (1:200), followed by fluorescently conjugated secondary antibodies, each for 1 h. For DAPI staining, 5 $\mu\text{g}/\text{ml}$ of the nuclear dye was added to the fixed and permeabilized cells, followed by incubation for 30 min at room temperature. Coverslips were mounted onto slides using DAKO™, left to dry overnight in the dark at room temperature, and then stored at -20°C .

Both live and fixed samples were analyzed by conventional epifluorescence microscopy using a Leica IRE DR2 inverted microscope with an Orca II ER camera (Hamamatsu) driven by the Openlab 3 software (Improvision) installed on an Apple G4 computer. Alternatively, analysis was made by confocal microscopy using a Zeiss LSM 510 laser scanning microscope with oil immersion objectives. Where indicated, the location of the plasma membrane was defined by addition of FM4-64 (20 μM) at the time of imaging. FM4-64 is a solvchromic red fluorescent dye that partitions into the outer monolayer of the plasmalemma. GFP, Cy3, and FM4-64 were examined using the conventional laser excitation lines and filter sets.

Online Supplemental Material

The online supplemental material (Figs. S1 and S2) is available at <http://www.jgp.org/cgi/content/full/jgp.200609656/DC1>. Fig. S1 shows the phosphoinositide changes induced by SigD. Lipids were extracted from HeLa cells after invasion by wild-type or SigD-deficient *Salmonella*. Lipids were analyzed for phosphoinositide content using HPLC. Fig. S2 shows the effect of SigD in renal epithelial cells. The expression of SigD was studied in opossum kidney (OK) cells. Morphological changes were studied alongside PtdIns(4,5)P₂ distribution as in Fig. 2.

RESULTS

SigD Hydrolyzes Phosphatidylinositol 4,5-Bisphosphate

SigD contains a domain with homology to mammalian inositol 4-phosphatases (Norris et al., 1998). We reported earlier that SigD induces the displacement of PLC δ -PH-GFP, a ligand of PtdIns(4,5)P₂, from the membrane of HeLa cells (Terebiznik et al. 2002) and interpreted these results to mean that the bacterial protein modified PtdIns(4,5)P₂ in a manner that rendered it unable to associate with the PH domain. However, SigD was also reported to act as an inositol polyphosphate phosphatase, capable of depleting cellular IP₆ and inositol pyrophosphates and of converting IP₅ into IP₄ (Norris

et al., 1998). The latter can in turn be converted to IP₃, which interacts with high affinity with PH domains. It was thus conceivable that the displacement of PLC δ -PH-GFP from the membrane occurred as a result of IP₃ formation, without alteration in PtdIns(4,5)P₂.

To determine whether SigD displays catalytic activity toward phosphoinositides *in vivo* we analyzed the lipid composition of HeLa cells exposed to the phosphatase using HPLC. Phosphoinositides were labeled using [³H]-myoinositol and the cells were otherwise untreated (control) or were infected with *Salmonella enterica* serovar Typhimurium (*S. Typhimurium*) to obtain extensive and nearly synchronous delivery of bacterial proteins to the host cell cytosol, via their type-III secretion system. Cells were infected with either wild type or with sigD-deficient *S. Typhimurium* (Δ sigD), in order to assess the contribution of the phosphatase. The inositide content data were normalized to the amount of PtdIns, the predominant species in mammalian cells, which is thought to be practically invariant. As shown in Table I, the PtdIns(4,5)P₂ content of control cells was equivalent to 8.2% of the PtdIns, in the range reported for other cells (Serunian et al., 1991). Infection for only 15 min with bacteria that express SigD (wild type) resulted in a 34% drop in the PtdIns(4,5)P₂ content, to 5.3% of the PtdIns. The decrease was consistently observed in three independent experiments and was statistically significant ($P < 0.05$ using ANOVA-Bonferroni's multiple comparison test). The large decrease in PtdIns(4,5)P₂ was absent when infection was performed using SigD-deficient bacteria (Table I). In this case, the drop was considerably smaller and not significant ($P > 0.05$).

The preceding data are consistent with the notion that SigD actively dephosphorylates PtdIns(4,5)P₂ to PtdInsP. This was confirmed by analyzing the PtdInsP content of the samples (Table I). In untreated cells the major PtdInsP peak detected by HPLC, which is comprised of PtdIns(4)P plus PtdIns(5)P, constituted 5.5% of the PtdIns. Infection with bacteria expressing SigD resulted in a considerable increase in PtdInsP, to 7.4% of PtdIns. Notice that the magnitude of the increase in PtdInsP is similar to the decrease in PtdIns(4,5)P₂ recorded under the same conditions, suggesting a precursor and product relationship. Importantly, the PtdInsP content was not increased when the cells were infected with SigD-deficient bacteria (Table I), confirming that the phosphatase is responsible for the generation of the inositide.

SigD Generates Phosphatidylinositol 5-Phosphate

Because SigD has homology to mammalian inositol 4-phosphatases (Norris et al. 1998), the disappearance of PtdIns(4,5)P₂ is likely the result of its conversion to phosphatidylinositol 5-phosphate (PtdIns(5)P). While the preceding data confirmed the near stoichiometric disappearance of PtdIns(4,5)P₂ and concomitant

appearance of PtdInsP, the HPLC system used is unable to differentiate PtdIns(5)P from phosphatidylinositol 4-phosphate (PtdIns(4)P). To test whether PtdIns(5)P is in fact formed we used a combined enzymatic and TLC assay that involves conversion of PtdIns(5)P to PtdIns(4,5)P₂ by PtdIns(5)P 4-kinase. The identity of the product of the enzymatic reaction was validated by HPLC (for details see Materials and methods and Morris et al. [2000] and Niebuhr et al. [2002]). As above, to discern the contribution of SigD we compared the effects of wild-type *Salmonella* to those of mutants devoid of SigD. The deletion of *sigD* was verified by immunoblotting (Fig. 1 B). As shown in Fig. 1 A, infection with wild-type, but not SigD-deficient *Salmonella*, generated a sizable amount of PtdIns(5)P, indicated by the formation of PtdIns(4,5)P₂. That this difference between the two bacterial strains was due to the deletion of *sigD* was confirmed by reintroduction of the phosphatase into the deficient *Salmonella*. Transformation of ($\Delta sigD$) *Salmonella* with a plasmid encoding wild-type SigD restored the production of PtdIns(5)P upon infection (Fig. 1 A). Like other active phosphatases, SigD has an essential cysteine in its active site. We generated a plasmid encoding a mutant SigD where the critical cysteine was replaced by serine, namely SigD (C462S). SigD-deficient bacteria were then transformed with this plasmid and used to infect mammalian cells. Immunoblotting was used to confirm that the level of expression of the mutant and wild-type forms of SigD was similar in the strains used (Fig. 1 B). Unlike the plasmid encoding wild-type SigD, the C462S mutant plasmid was unable to restore the appearance of PtdIns(5)P (Fig. 1 C), confirming that the 4-phosphatase activity of the enzyme is responsible, at least in part, for the hydrolysis of PtdIns(4,5)P₂.

In principle, PtdIns(5)P could have also been generated by dephosphorylation of PtdIns(3,5)P₂ on position 3, as has been reported for myotubularins (Tronchere et al., 2004), or by sequential dual dephosphorylation of PtdIns(3,4,5)P₃, a preferred substrate of SigD in vitro (Norris et al., 1998). Several lines of evidence argue against these possibilities. First, analysis by HPLC revealed that the cellular content of PtdIns(3,5)P₂ is far too low to account for the increase in PtdInsP. As shown in Fig. S1 A (available at <http://www.jgp.org/cgi/content/full/jgp.200609656>), the basal level of PtdIns(3,5)P₂ is equivalent to $\approx 0.1\%$ of the PtdIns, over 25 times lower than the increase in PtdInsP recorded in the same experiments. It is unlikely that PtdIns(3,5)P₂ is rapidly generated by other processes and simultaneously degraded by SigD, thus failing to accumulate. This is indicated by the finding that the PtdIns(3,5)P₂ content of cells infected with SigD-deficient bacteria is also extremely low, similar to that of untreated or wild-type *Salmonella*-infected cells (Fig. S1 A). Like PtdIns(3,5)P₂, the content of PtdIns(3,4,5)P₃ in resting cells is much too low ($\approx 0.1\%$ of PtdIns) to account for the formation

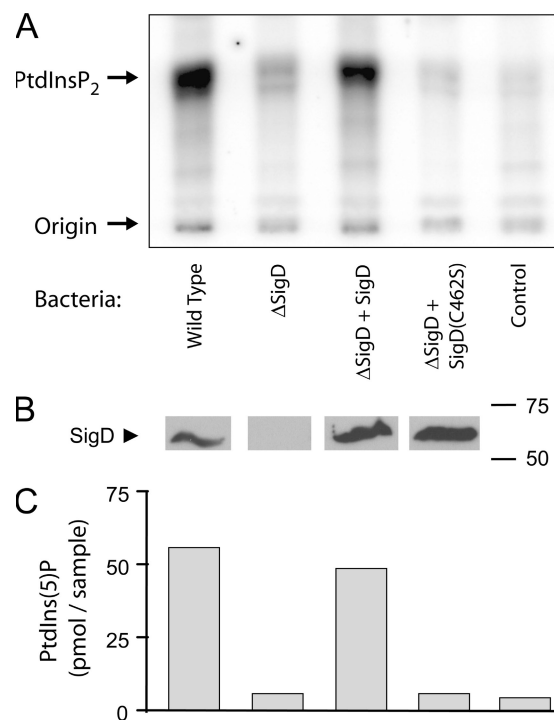


Figure 1. Generation of PtdIns(5)P by SigD. HeLa cells were infected with the indicated strains of *Salmonella* and, after 10 min at 37°C, the reaction was stopped and lipids were extracted as described in Materials and methods. The PtdIns(5)P content was next analyzed by its enzymatic conversion to radiolabeled PtdIns(4,5)P₂ by insertion of the gamma phosphate of [³²P]ATP, catalyzed by the type II phosphoinositide kinase, which selectively phosphorylates the 4'-position of PtdIns(5)P. The resulting lipids were next separated by thin layer chromatography. A representative chromatogram is shown in A. The site where the lipid mixture was spotted (Origin) and the position of the PtdIns(4,5)P₂ produced are indicated. The cells were infected, from left to right, with wild-type *Salmonella*, SigD-deficient *Salmonella*, SigD-deficient *Salmonella* bearing a plasmid expressing wild-type SigD cDNA, and SigD-deficient *Salmonella* bearing a plasmid expressing the catalytically inactive SigD mutant SigD (C462S). Lipids from uninfected cells are shown in the last lane. The deletion of SigD and the level of expression of the retransformed wild-type and mutant SigD were verified by immunoblotting. Identical amounts of bacteria were loaded, and lanes from the same gel and exposure are shown in B, which is representative of two similar blots. Lanes were separated in the image to facilitate alignment with the TLC (above) and bar graph (below). Molecular mass markers (in kD) are shown to the right. In C the amount of PtdIns(4,5)P₂ present in each TLC sample was quantified by HPLC and online continuous-flow liquid-scintillation counting. The chromatogram and quantitation shown are representative of three similar independent experiments.

of PtdInsP, did not decrease upon infection with wild-type bacteria, and did not increase in cells infected with ($\Delta sigD$) bacteria (unpublished data).

Additional evidence against the involvement of PtdIns(3,5)P₂ or PtdIns(3,4,5)P₃ in the generation of PtdIns(5)P was obtained using LY294002. This compound effectively inhibits both class I and class III PtdIns 3 kinases, which are required for the formation

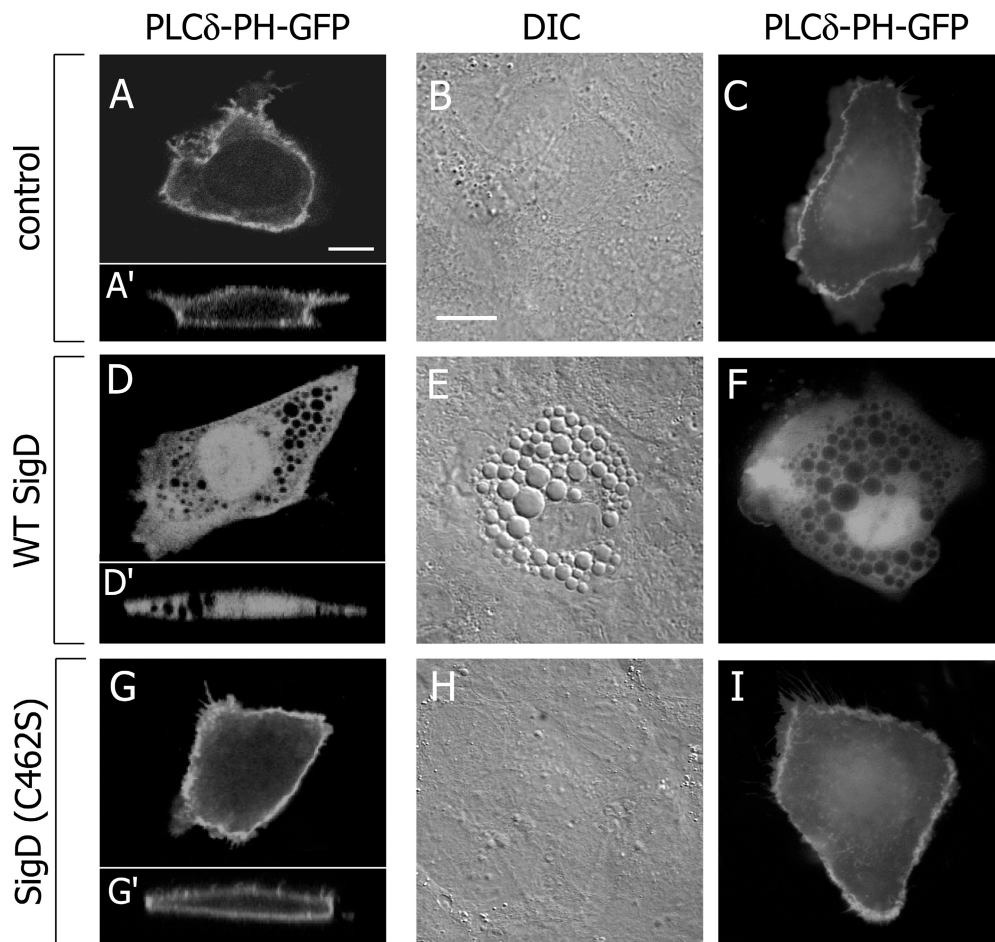


Figure 2. Effect of SigD on PtdIns(4,5)P₂ distribution and cellular morphology. Intestinal epithelial cells (IEC-18) were microinjected with cDNA encoding PLCδ-PH-GFP only (A–C), or together with either wild-type SigD (D–F) or SigD (C462S) cDNA (G–I). Cells were then incubated for 3 h at 37°C before imaging by confocal (A, D, and G), differential interference contrast (DIC; B, E, and H), or conventional epifluorescence microscopy (C, F and I). A, D, and G illustrate representative x vs. y confocal slices acquired near the middle of the cell, while A', D', and G' are the corresponding x vs. z reconstructions. The DIC images in B, E, and H correspond to the cells in C, F, and I, respectively. The images are representative of at least 10 similar experiments of each type. Bar, 10 μm.

of PtdIns(3,4,5)P₃ and of PtdIns(3)P, the precursor of PtdIns(3,5)P₂, respectively. Fig. S1 B shows that under the conditions used, LY294002 blocked PtdIns 3-kinase activity; endosomal PtdIns(3)P, detected using a tandem FYVE domain from EEA1, disappeared upon treatment with the drug (panels B and B'). When cells were first treated with LY294002 and then infected with wild-type *Salmonella* in the presence of the inhibitor, the generation of PtdIns(5)P persisted (Fig. S1 C).

Jointly, these observations provide convincing evidence that SigD from *Salmonella* is an effective phosphoinositide phosphatase capable of converting PtdIns(4,5)P₂ to PtdIns(5)P. Whether the increase in PtdInsP measured by HPLC can be accounted for in its entirety by PtdIns(5)P remains to be defined, since the combined enzymatic/TLC assay does not yield quantitative estimates. Nevertheless, it is clear that at least a fraction of the PtdInsP generated is PtdIns(5)P.

Effect of SigD on the PtdIns(4,5)P₂ Content of Epithelial Cells

The IEC-18 cell line was used as an epithelial model for these studies for two reasons. First, it forms well-defined polarized monolayers with distinct junctional complexes (see below). Second, IEC-18 cells were derived

from the small intestine, where *Salmonella* infection occurs in humans. Thus, our studies could potentially yield both basic and pathophysiological information. Confluent epithelial monolayers are notoriously difficult to transfect, and this was found to be the case for IEC-18 cells as well (unpublished data). To introduce cDNA into these cells without disrupting the integrity of the monolayer we opted instead to use microinjection. The number of cells that can be injected precluded biochemical analyses but provided reproducible results when single cells were analyzed microscopically.

The PH domain of PLCδ has been used extensively to monitor PtdIns(4,5)P₂ in live cells (Stauffer et al., 1998; Raucher et al., 2000; Varnai et al., 2002). The distribution of PLCδ-PH-GFP expressed in IEC-18 cells is illustrated in Fig. 2 (A–C). As anticipated from its association with PtdIns(4,5)P₂, the construct is mostly bound to the inner aspect of the plasma membrane. Both the apical and basolateral membranes were comparably labeled (see z-axis reconstruction in Fig. 2 A'). The plasmalemmal association of PLCδ-PH-GFP is best visualized by confocal microscopy (Fig. 2 A) but can be readily appreciated also by conventional fluorescence microscopy (Fig. 2 C). Note that microinjection and expression of PLCδ-PH-GFP had no discernible effect on

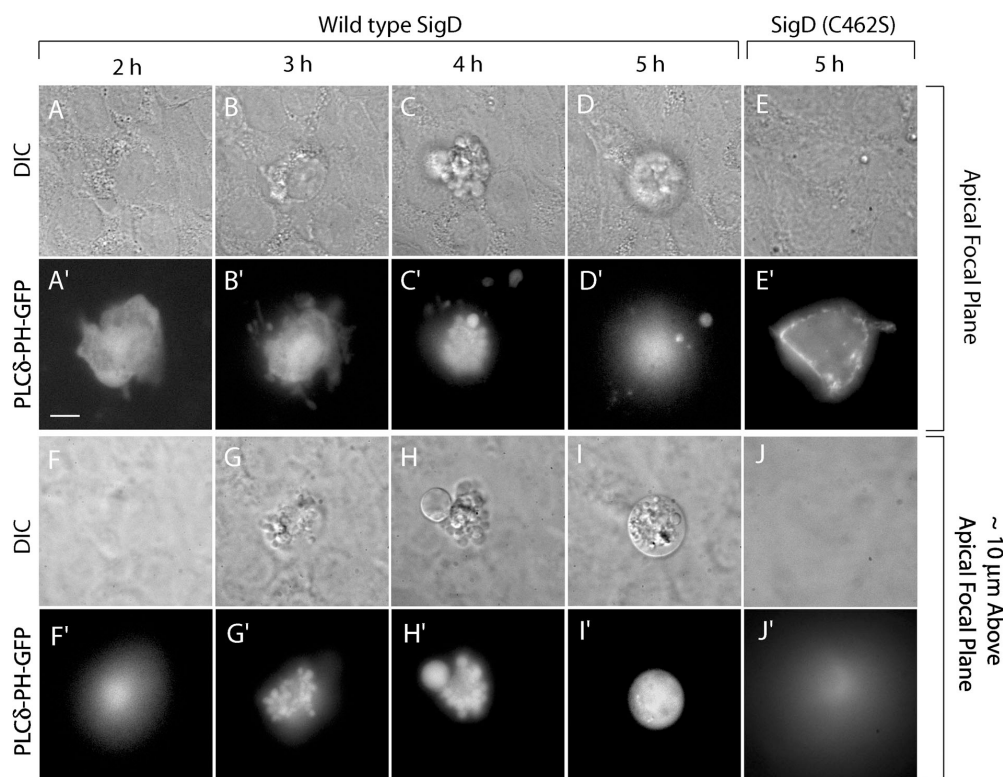


Figure 3. Time course of the effects of PtdIns(4,5)P₂ depletion on epithelial morphology. Epithelial cells grown to confluence were used for microinjection of PLCδ-PH-GFP and SigD cDNA (1:5 ratio). Wild-type SigD was used in A–D and F–I, while SigD (C462S) was used in E and J. DIC and epifluorescence images were acquired with the focal plane near the apical surface of the cells (A–E) or ≈10 μm above the apical membrane (F–J). The images shown are representative of at least five similar experiments. Bar, 10 μm.

IEC-18 cell morphology, as is evident from DIC microscopy (Fig. 2 B).

The effect of SigD on PLCδ-PH-GFP distribution is shown in Fig. 2 (D–F). As early as 1 h after microinjection the phosphatase reverted the association of PLCδ-PH-GFP with the membrane, rendering the construct largely cytosolic. The displacement was evident both by confocal (Fig. 2 D) and conventional microscopy (Fig. 2 F). Line scans of images like those in Fig. 2 (A and D), followed by densitometry of the resulting scans were used to quantify the reproducibility and statistical significance of the effect of SigD. The pixel density at the membrane, defined by staining with FM4-64, was normalized to that of the cytosol. In seven similar determinations the membrane-to-cytosol ratio averaged 7.97 ± 1.4 , while in SigD-treated cells it was 0.97 ± 0.01 (data are mean values \pm SEM). This difference is highly significant ($P < 0.001$). DIC imaging of SigD-injected cells revealed that they underwent extensive vacuolation, and fluorescence microscopy indicated that these vacuoles are sealed, as they excluded PLCδ-PH-GFP. That the displacement of PLCδ-PH-GFP is due to the phosphatase activity of SigD was ascertained by microinjecting SigD(C462S). The inactive mutant had no detectable effect on the distribution of PLCδ-PH-GFP and failed to produce vacuolation (Fig. 2, G–I). Indeed, SigD(C462S)-injected cells were indistinguishable from the controls, implying that all the observed effects of wild-type SigD are attributable to its phosphoinositide phosphatase activity.

The effects of SigD were not restricted to intestinal epithelial cells, but were observed also in renal epithelial cells. The accumulation of PLCδ-PH-GFP at the plasmalemma and its displacement by SigD were noted also in OK cells, an opossum kidney line (see Fig. S2). Together, the results of Fig. 2 and Fig. S2 confirm the effectiveness of SigD as a phosphoinositide phosphatase when introduced into mammalian cells and highlight its ability to deplete PtdIns(4,5)P₂ in epithelial cells.

Effect of SigD on Epithelial Morphology and Integrity

In addition to the vacuolation reported in Fig. 2, other structural changes were consistently noted in cells expressing SigD. These changes developed gradually over time and were always preceded by displacement of PLCδ-PH-GFP from the membrane, suggesting that they were a consequence of the hydrolysis of PtdIns(4,5)P₂. The development of the structural changes is illustrated in Fig. 3. Concomitantly with the appearance of vacuoles, cells injected with SigD extend lamellipodia beyond the original junctional complexes (see Fig. 3, B and B', and Fig. 4 below). At later times blebbing of the apical surface is apparent (Fig. 3, C and C'). These blebs extend well beyond the surface of the monolayer and are in fact best detected when the focal plane of the microscope is raised by 10 μm above the normal apical surface (Figs. 3, H and H'). Eventually, most of the PtdIns(4,5)P₂-depleted cell bulges above the monolayer, rounding up (Fig. 3, D–I) and finally detaching from the epithelium. All of these effects depend on the

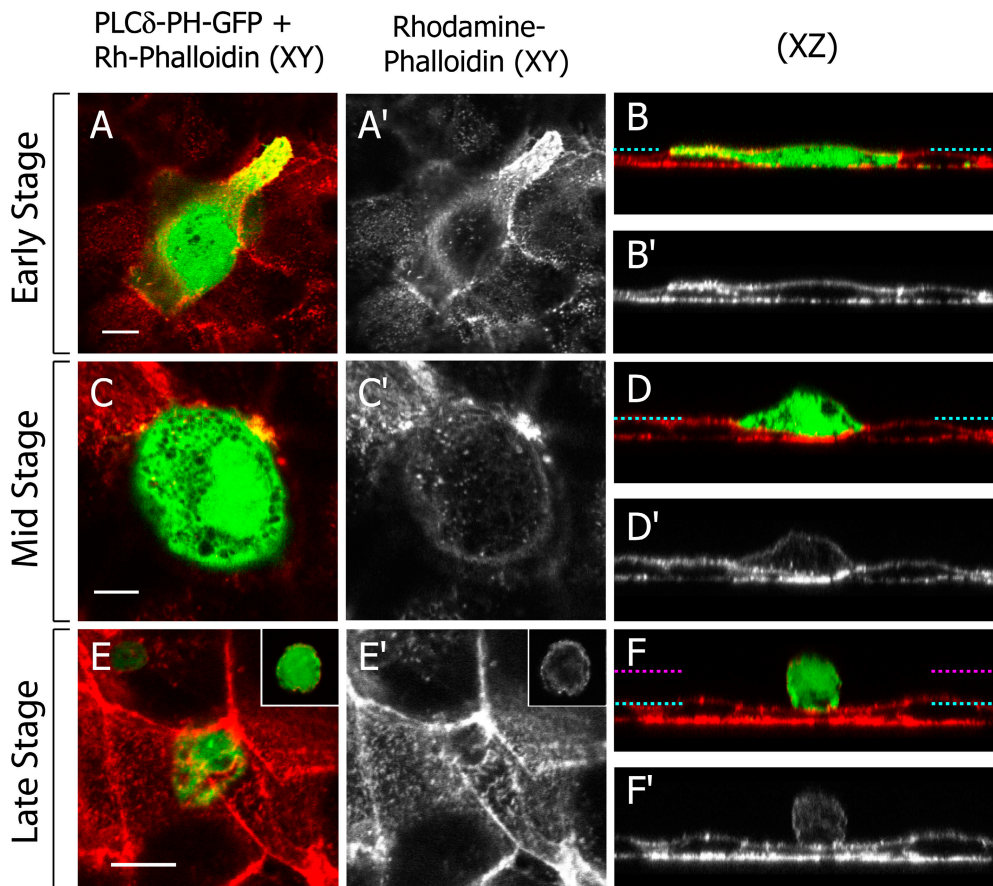


Figure 4. Effect of PtdIns(4,5) P_2 depletion on F-actin and PtdIns(4,5) P_2 distribution. Intestinal epithelial cells (IEC-18) were microinjected with PLC δ -PH-GFP and SigD cDNA (1:5 ratio). The monolayers were incubated for varying periods of time and were then fixed, permeabilized, and stained with rhodamine-phalloidin to reveal F-actin. The stained cells were then analyzed by confocal fluorescence microscopy. Panels A–F show PLC δ -PH-GFP in green and F-actin in red. Panels A'–F' show only F-actin in white. Panels A, A', C, C', E, and E' illustrate representative x vs. y confocal slices acquired near the middle of the cell, while B, B', D, D', F, and F' are the corresponding x vs. z reconstructions. A and B are representative of cells fixed at an early stage, i.e., 2–4 h after injection. C and D are representative of cells fixed at an intermediate stage, i.e., 4–5 h after injection. E and F are representative of cells fixed at a late stage, i.e., 5–6 h after injection. The images shown are representative of 10 similar experiments of each type. Bar, 10 μ m.

phosphatase activity of SigD, since they were never observed in cells expressing SigD(C462S). As shown in Fig. 3 (E and J), such cells retained normal morphology and remained as integral components of the monolayer even after 5 h, when cells expressing wild-type SigD had generally bulged and rounded up.

Because PtdIns(4,5) P_2 effectively modulates the actin cytoskeleton, we speculated that the morphological changes induced by SigD were due, at least in part, to alterations in actin filament structure. To test this notion cells were fixed and permeabilized at various times after microinjection with cDNA encoding SigD and PLC δ -PH-GFP. The cells were then stained with rhodamine-phalloidin to reveal F-actin and analyzed by confocal microscopy (Fig. 4). These experiments indicated that actin underwent a biphasic change. At the early stages of action of SigD, the F-actin content of the cells seemingly increased, particularly in the lamellipodia that extended beyond the normal junctional boundaries (Fig. 4, A and B). At this stage, the SigD-injected cells remained within the context of the monolayer, though the stress fibers attaching them to the substratum were somewhat depleted (not depicted). Subsequently,

bulging above the monolayer and vacuolation became apparent (panels C and D, labeled “mid-stage” in Fig. 4). At this time the lamellipodia had receded and the net F-actin content of the cells had diminished. At even later stages the vacuoles were resorbed and the cells rounded up and protruded above the monolayer (Fig. 4, E and F, labeled “late stage”), ultimately detaching. Little F-actin remained at this stage, accounting for cell rounding. Of note, the neighboring cells rapidly occupied the space vacated by the PtdIns(4,5) P_2 -depleted cell, a form of epithelial restitution.

The Effects of SigD on the Cytoskeleton Are Mediated by Depletion of PtdIns(4,5) P_2

As described above, the structural changes elicited by SigD were not mimicked by SigD(C462S). Because this inactive mutant also failed to alter PtdIns(4,5) P_2 , depletion of the inositide is likely responsible for the observed structural changes. However, it is also possible that accumulation of PtdIns(5)P is involved and, since SigD hydrolyzes several soluble inositol phosphates (Norris et al., 1998), generation of IP $_4$ from IP $_5$ is another potential cause of the morphological changes.

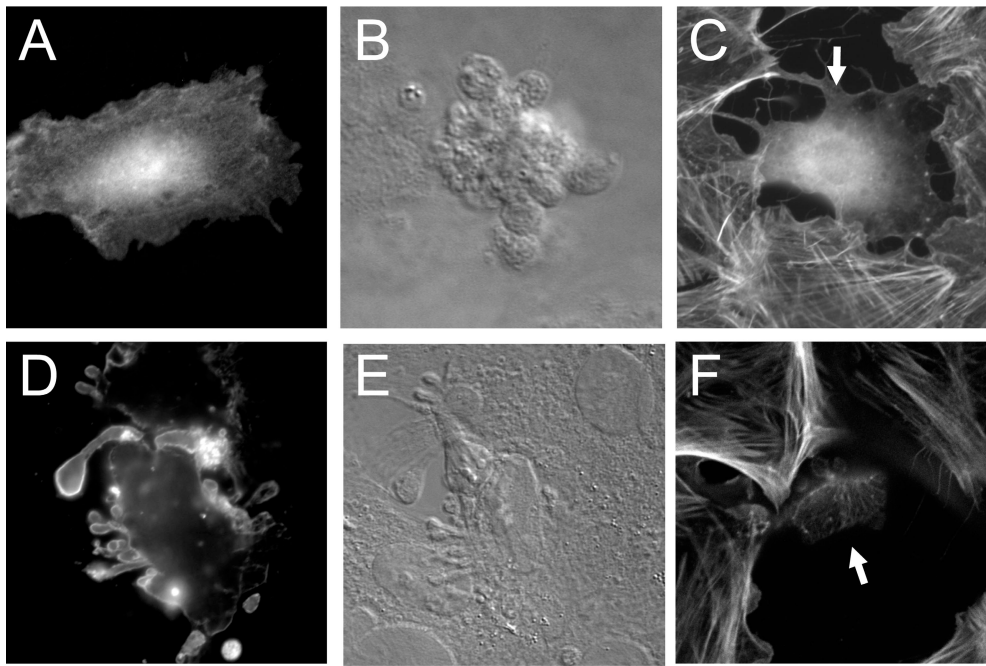


Figure 5. Alternative means of regulating $\text{PtdIns}(4,5)\text{P}_2$. IEC-18 cells were microinjected with cDNA encoding for (A–C) the phosphatase domain of synaptojanin-2 fused to a CAAX box (PD-CAAX), or (D–F) two tandem copies of the PH domain of PLC δ -PH fused to GFP (see Materials and methods for details regarding use and construction). In A, the PD-CAAX DNA was coexpressed with the PLC δ -PH-GFP to identify transfected cells and to ensure the $\text{PtdIns}(4,5)\text{P}_2$ hydrolysis occurred. (A and D) Green fluorescence; (B and E) DIC images. The cell in D corresponds to E; (C and F) actin staining using phalloidin. Arrows indicate injected cells.

The latter possibility was analyzed by directly microinjecting the cells with IP_4 . The concentration of IP_4 in the injection pipette was 100 μM . Because we estimate that the injection volume approximates 5–10% of the total cell volume, a final concentration of 5–10 μM IP_4 must have been delivered to the cells. This concentration is higher than the concentration of IP_4 reported in cells infected by *Salmonella* (Zhou et al., 2001). In four experiments, injection of IP_4 had no discernible effect on IEC-18 cell morphology or association with the monolayer (unpublished data). Similarly, microinjection of $\text{PtdIns}(5)\text{P}$ or extracellular addition of this lipid in the presence of carriers that facilitate intracellular delivery of inositides was without effect on cell morphology (unpublished data).

These observations suggest that depletion of $\text{PtdIns}(4,5)\text{P}_2$, not production of $\text{PtdIns}(5)\text{P}$ or IP_4 , was the cause of the morphological changes. To validate this conclusion, we manipulated $\text{PtdIns}(4,5)\text{P}_2$ by two independent procedures. First, we transfected a phosphoinositide phosphatase of mammalian origin, synaptojanin-2. To improve the efficiency of hydrolysis, a construct encoding the phosphatase domain was targeted to the membrane by addition of a prenylation motif, a polycationic sequence and CAAX box modeled after the C terminus of K-Ras. Expression of this construct effectively displaced PLC δ -PH-GFP from the membrane (Fig. 5 A; see Fig. 2 A for comparison with untreated control), indicating hydrolysis of $\text{PtdIns}(4,5)\text{P}_2$. More prolonged expression of the synaptojanin-2 phosphatase-CAAX construct induced cell blebbing (Fig. 5 B) and eventual detachment of the cells from the substratum. In parallel, the actin cytoskeleton was drastically

altered, with marked disappearance of stress fibers (Fig. 5 C).

We also tested the effects of overexpression of an avid $\text{PtdIns}(4,5)\text{P}_2$ ligand, which at sufficiently high concentrations should mask a significant fraction of the inositolide. To this end we used a construct of two tandem copies of the PH domain of PLC δ , which is predicted to have enhanced avidity for $\text{PtdIns}(4,5)\text{P}_2$. As shown in Fig. 5 D, 2(PLC δ -PH)-GFP binds very effectively to the plasmalemmal $\text{PtdIns}(4,5)\text{P}_2$ and, when expressed at high levels, induced cell blebbing (Fig. 5, D and E) and pronounced changes in cytoskeletal architecture (Fig. 5 F). Because the structural changes produced by synaptojanin-2 phosphatase-CAAX and 2(PLC δ -PH)-GFP resemble those induced by SigD, we believe that diminution in the amount of available plasmalemmal $\text{PtdIns}(4,5)\text{P}_2$ is the common underlying mechanism.

Effect of $\text{PtdIns}(4,5)\text{P}_2$ Depletion on Tight Junction Integrity

Since tight junctions are necessary to maintain epithelial integrity, which was lost upon expression of SigD, we suspected that depletion of $\text{PtdIns}(4,5)\text{P}_2$ may have destabilized the junctional complexes. This was tested by staining control and transfected monolayers with antibodies to ZO-1, a well-established tight junction marker. As reported earlier (Ma et al., 1992), in confluent monolayers of IEC-18 cells ZO-1 was found to line the cellular junctions in a virtually continuous pattern (Fig. 6 A). Similar results were obtained in cells injected only with soluble or membrane-associated GFP constructs used as indicators of expression (not illustrated). Even at the early stages of the $\text{PtdIns}(4,5)\text{P}_2$ depletion process

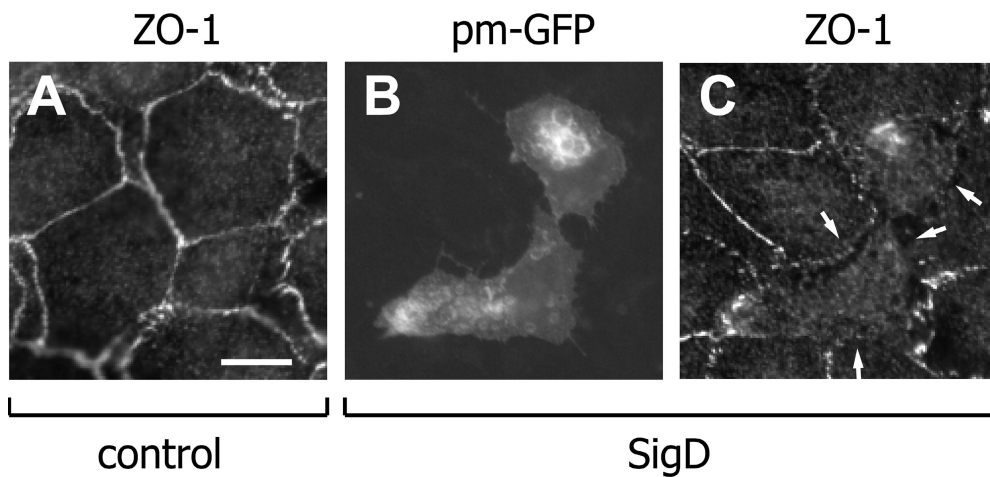


Figure 6. Effect of PtdIns(4,5) P_2 depletion on junctional integrity. Intestinal epithelial cells (IEC-18) were either untreated (A) or were microinjected with PM-GFP, a fluorescent microinjection and expression marker together with SigD cDNA (B and C). The monolayer was incubated for 2 h to allow expression and then fixed, permeabilized, and stained with antibodies to ZO-1, followed by Cy3-coupled secondary antibodies. The cells were analyzed by fluorescence microscopy. Red fluorescence is shown in A and C and green in B. Arrows point to regions where junctional staining is discontinuous. Images are representative of five similar experiments. Bar, 10 μ m.

(1–3 h after injection) disruption of the junctional integrity was apparent, as judged by the discontinuities in the ZO-1-staining pattern (Fig. 6, B and C). Preferential staining with ZO-1 at the cell boundary was completely eliminated at later stages. A disruption of ZO-1 architecture was also observed in cells expressing the synaptotagmin-CAAX construct as well as in cells with high levels of 2(PLC δ -PH)-GFP expression. Importantly, the effect of SigD injection on junctional integrity was absent when the phosphatase-inactive mutant SigD(C462S) was used (unpublished data), pointing to depletion of PtdIns(4,5) P_2 as the underlying mechanism.

Does SigD Induce Apoptosis of Epithelial Cells?

The blebbing and rounding observed in cells expressing SigD is also characteristic of apoptotic cells (Majno and Joris, 1995). Moreover, infection with *Salmonella* has been reported to promote apoptosis of some cell types (Knodler and Finlay, 2001). It was therefore important to establish whether depletion of PtdIns(4,5) P_2 by SigD sufficed to trigger programmed cell death in IEC-18 cells. To this end, cells were coinjected with SigD or SigD(C462S) and a fluorescent protein, used as an injection and expression marker. Apoptosis was initially assessed from nuclear morphology in cells stained with DAPI. A very small fraction of the uninjected cells (1–2%) had an apoptotic phenotype, consistent with findings in other cells (Majno and Joris, 1995). The sensitivity of the detection procedure was validated treating the cells with 100 nM of staurosporine for 2 or 5 h, which increased the apoptotic index to 13.4% and 34.9%, respectively. More importantly, when comparing over 100 cells from three experiments no significant increase

in the fraction of apoptotic cells was detected in SigD-expressing cells (2%), even at the longest times tested. Longer times were not investigated, as the cells tended to detach from the monolayer (see Fig. 3).

DAPI staining is simple, yet not the most sensitive method for detection of apoptosis. Gross changes in nuclear morphology occur only in advanced stages of apoptosis and the time window of our experiments may have been insufficient to reach such stages. For this reason, we also assessed apoptosis using a more sensitive method that detects earlier stages of programmed cell death. Control and SigD-expressing cells were stained with a specific antibody that recognizes the activated form of caspase-3, an essential early component of the apoptotic chain. As in the case of DAPI, no significant difference in the fraction of apoptotic profiles was measured in four determinations between control and SigD-expressing cells (2% vs. 1%) while distinct apoptosis was observed following a short treatment with staurosporine (10.5% after 2 h). Jointly, these experiments indicate that apoptosis is not prevalent during the first 4–6 h of expression of SigD, at a time when PtdIns(4,5) P_2 is extensively degraded and cell morphology is drastically altered. These results are consistent with the findings of Santos et al. (2001), who determined that SigD was not required for the induction of apoptosis in host cells in an animal model of *Salmonella* infection.

Effect of PtdIns(4,5) P_2 Depletion on Anion Permeability

In the context of the intestinal epithelium, transient opening of the junctional complexes would be predicted to result in loss of vectorial ion transport and possibly cause diarrhea (Uzzau and Fasano, 2000). Indeed,

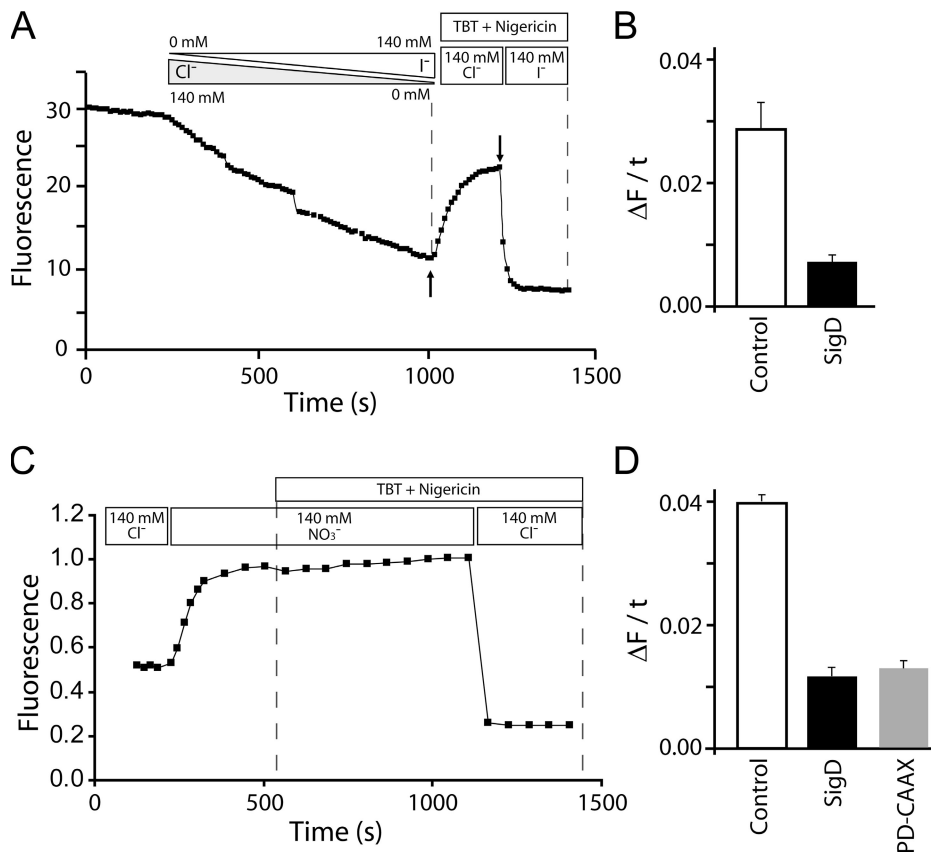


Figure 7. Effect of PtdIns(4,5)P2 depletion on anion permeability. (A and B) IEC-18 cells were microinjected with YFP(H148Q), a halide-sensitive fluorescent protein with or without wild-type SigD cDNA. The cells were allowed to express the fluorescent probe for 2 h and subjected to digital imaging for assessment of halide permeability as described under Materials and methods. (A) Representative experiment. The emission of YFP(H148Q) is shown over time in a cell not expressing SigD. Where indicated, the concentration of chloride in the bathing medium was reduced by isoosmotic replacement with iodide. For calibration, the cells were permeabilized using tributyltin (TBT) and nigericin. (B) Quantitation of relative chloride permeability in cells expressing either YFP(H148Q) alone (control) or in combination with SigD. The rate of change of the fluorescence over time ($\Delta F/t$) was calculated following reduction of chloride to 0 mM by isoosmotic replacement with iodide. To allow comparison between experiments the fluorescence was normalized to the initial (maximal) value. Data are means \pm SEM of 11 individual

cells from three separate experiments. (C and D) Cells were microinjected with SigD cDNA as above or alternatively with the PD-CAAX construct and subsequently loaded hypotonically with MQAE as detailed in Materials and methods. Following a 30-min recovery period, the chloride concentration was manipulated using nitrate as a substitute and calibrated as in A. (D) Quantitation of the rate of change of MQAE fluorescence over time in control cells (open bar) with SigD (filled bar) or with PD-CAAX (gray bar). Data are means \pm SEM of 121 cells from three separate experiments.

SigD has been identified as a principal factor in causing diarrhea in animal models of *Salmonella* infection (Galyov et al., 1997). However, the loss of fluid was not attributed to loss of junctional integrity, but was instead proposed to be caused by increased Cl^- secretion in response to elevated levels of IP_4 (Norris et al., 1998). This conclusion, however, was derived from studies of chloride influx into nonepithelial (HEK293) cells and required validation in epithelia.

We implemented measurements of anion permeability using a novel halide-responsive variant of the yellow fluorescent protein, YFP(H148Q). This protein responds to variations in halide concentration with changes in pK_a that, at constant pH, translate into fluorescence changes (Jayaraman et al., 2000). IEC-18 cells were microinjected with the cDNA encoding YFP(H148Q), together with or without SigD. A typical measurement is illustrated in Fig. 7 A, where the concentration of Cl^- in the medium was varied stepwise, by isoosmotic replacement with I^- . The latter anion is a more effective quencher of YFP(H148Q) emission, resulting in a progressive diminution of fluorescence. The loss was largely, but not entirely reversible, due to

photobleaching incurred during repeated acquisitions. Indeed, a comparable partial decrease was noted upon repeated illumination at constant $[\text{Cl}^-]$. The bleaching component could be readily interpolated and corrected in our measurements. Finally, tributyltin and nigericin were used to calibrate the fluorescence vs. $[\text{Cl}^-]$. Using this approach, we were able to compare the rates of halide exchange in control cells and in cells expressing SigD. Cells were tested at the early and mid stages of expression, but not at the late stages (see Fig. 3), because the tenuous attachment of the latter to the monolayer made measurements unreliable and calibration impossible. The data collected from 11 determinations are summarized in Fig. 7 B. Contrary to the predictions made on the basis of the work of Feng et al. (2001), we found that halide permeability was in fact depressed by SigD.

Because GFP-derived probes such as YFP(H148Q) can be affected by environmental parameters other than the halide concentration, including the pH, it was imperative to ascertain that this unexpected discrepancy did not result from an experimental artifact. We therefore performed an independent set of experiments using a

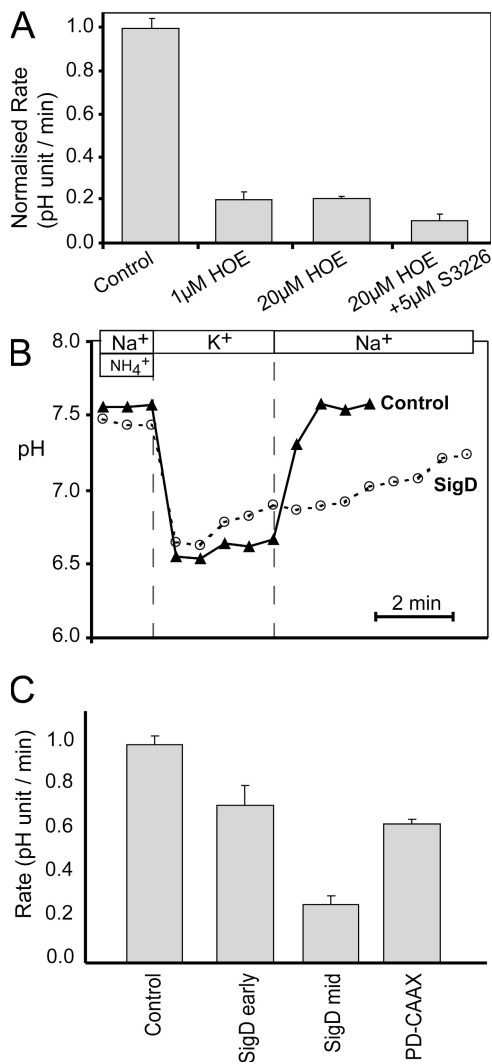


Figure 8. Effect of PtdIns(4,5)P₂ depletion on pH regulation. To measure pH, IEC-18 cells were microinjected with YFP cDNA with or without wild-type SigD cDNA. The cells were allowed to express the proteins for 2 h. Alternatively, cells microinjected with PLCδ-PH-GFP with or without wild-type SigD or PD-CAAX cDNA were loaded with SNARF-5F during the final 30 min of the expression period. The cells were then subjected to digital imaging for assessment of cytosolic pH, as described under Materials and methods. (A) To define the functional contribution of individual NHE isoforms, the rate of pH recovery was measured in SNARF-5F-loaded cells treated with the indicated inhibitors. From left: untreated cells; cells treated with 1 µM HOE694 (expected to inhibit NHE1 almost exclusively); cells treated with 20 µM HOE694 (expected to inhibit both NHE1 and NHE2); cells treated with 20 µM HOE694 plus 5 µM S3226 (expected to inhibit NHE1, NHE2 and NHE3). (B) Representative experiment showing pH recovery from an acid load in YFP (solid triangles) and YFP plus SigD-expressing cells (open circles). The emission of YFP was calibrated using nigericin and potassium, and the pH determined from such calibrations is shown over time. The cells were prepulsed with ammonium to induce cytosolic acidification upon its removal. Where indicated, sodium in the bathing medium was replaced isoosmotically by potassium and vice versa. (C) Quantitation of relative Na⁺/H⁺ exchange activity of control, SigD-expressing, or PD-CAAX-expressing cells. Activity was measured as the rate of sodium-induced pH recovery, measured

different chloride-sensitive probe, MQAE. While sensitive to halide concentrations, MQAE fluorescence is not altered by the physiological anions HCO₃⁻, SO₄²⁻, and PO₄³⁻, by cations, or by pH (Verkman et al., 1989). Results of a typical experiment are shown in Fig. 7 C and the summary of 10 determinations from three separate experiments is presented in Fig. 7 D. As found using YFP(H148Q), the MQAE results indicate that anion permeability is diminished by treatment with SigD. To ensure that this diminution was caused by hydrolysis of PtdIns(4,5)P₂, as opposed to dephosphorylation of inositol polyphosphates, we also tested the effects of PD-CAAX on chloride permeability. As shown in Fig. 7 D (gray bar), this membrane-associated, phosphoinositide-specific phosphatase produced an inhibition comparable to that seen with SigD, ruling out mediation by hydrolysis of soluble inositol polyphosphates. These findings are not consistent with elevated Cl⁻ secretion as the mechanism underlying SigD-induced diarrhea and, in addition, suggest a role for PtdIns(4,5)P₂ in the modulation of epithelial anion transport.

Effect of PtdIns(4,5)P₂ Depletion on Na⁺/H⁺ Exchange

The apical membranes of intestinal and renal epithelial cells are active sites of Na⁺ resorption. Much of this absorption occurs in exchange for H⁺ and is coupled to Cl⁻/HCO₃⁻ exchange and to osmotically obliged fluid absorption. There is evidence in model systems that some isoforms of the NHE are sensitive to the concentration of PtdIns(4,5)P₂ (Aharonovitz et al., 2000; Fuster et al., 2004), though this has not been validated for epithelial cells. The possible regulation of epithelial exchangers by PtdIns(4,5)P₂ is important not only in the context of *Salmonella* infection, but also because PtdIns(4,5)P₂ can vary during signaling, changes in cell volume, and ischemia. We therefore took advantage of the selective phosphatase activity of SigD and PD-CAAX to investigate the specific effects of PtdIns(4,5)P₂ depletion on Na⁺/H⁺ exchange activity in epithelial cells.

Epithelial cells often coexpress multiple isoforms of NHE. To our knowledge, the isoforms present in IEC-18 cells have not been defined. Therefore, we first assessed the overall NHE activity of these cells and estimated the contribution of the “housekeeping” NHE1 isoform and of specialized isoforms like NHE2 and NHE3. NHE activity was assessed as the Na⁺-induced recovery of the cytosolic pH from an acid load. Cytosolic acidification was imposed using an ammonium prepulse, as previously described (Aharonovitz et al., 2000). Preliminary experiments revealed that IEC-18 cells have a robust exchange activity (Fig. 8 A, a sample trace is shown in B, triangles).

over the first 1–2 min. Data show rates of alkalization and are means ± SEM of at least three experiments of each type.

The contribution of individual isoforms to this response was investigated using HOE694, an inhibitor that differentially affects various NHE isoforms. At low ($\leq 1 \mu\text{M}$) concentrations, HOE694 selectively blocks NHE1, while at higher concentrations ($20 \mu\text{M}$) it also blocks NHE2. Under these conditions, NHE3 is largely unaffected (Counillon et al., 1993). A different inhibitor has the converse effect; at $5 \mu\text{M}$ S3226 preferentially inhibits NHE3. As shown in Fig. 8 A, 82% of Na^+/H^+ exchange in IEC-18 cells was blocked by $1 \mu\text{M}$ HOE694. The fractional inhibition was not increased when $20 \mu\text{M}$ HOE694 was used, but an additional 11% was inhibited when $5 \mu\text{M}$ S3226 was added. These findings imply that Na^+/H^+ exchange in IEC-18 cells is largely mediated by NHE1, with a smaller contribution by NHE3. No NHE2 activity was detectable in these cells.

We proceeded to assess the effect of $\text{PtdIns}(4,5)\text{P}_2$ depletion on exchange activity. As for Cl^- determinations, cells were tested at early and mid stages of expression, but not at the late stages, because the tenuous attachment of the latter to the monolayer made calibration impossible. Indeed, late stage cells become permeant to H^+ equivalents and could not be acid loaded to the same degree as control cells. As illustrated in Fig. 8 (B and C), depletion of $\text{PtdIns}(4,5)\text{P}_2$ by expression of SigD produced inhibition of NHE activity, which became more pronounced at the later stages of expression of this phosphatase. A significant inhibition of the antiport was also observed when cells were transfected with PD-CAAX, confirming that physiological $\text{PtdIns}(4,5)\text{P}_2$ levels are required for optimal NHE activity. These findings are in accord with the inositide sensitivity reported in nonepithelial model systems expressing NHE1 (Aharonovitz et al., 2000; Fuster et al., 2004) and NHE3 (Fuster et al., 2004).

DISCUSSION

SigD Is a $\text{PtdIns}(4,5)\text{P}_2$ Phosphatase

The biological activity of SigD was first inferred from its sequence homology with mammalian phosphoinositol phosphatases (Norris et al., 1998). Its ability to dephosphorylate inositol phosphates was then demonstrated in vitro and cells expressing SigD were found to accumulate IP_4 . It was subsequently appreciated, however, that SigD is largely membrane bound (Marcus et al., 2002), not an ideal location for the degradation of soluble substrates. Its subcellular location suggested that the degradation of inositol phosphates may not be the sole or even the most important function of SigD and prompted investigators to test whether it can additionally hydrolyze phosphoinositides. This notion was tested by in vitro experiments that were met with positive, yet conflicting, results; different groups confirmed that SigD is active against phospholipids, but the substrate

selectivity varied among reports (Norris et al. 1998; Marcus et al., 2001; Hernandez et al., 2004).

The first indication that SigD effectively cleaves phospholipids when introduced into mammalian cells was provided by Terebiznik et al. (2002), who described dissociation of $\text{PLC}\delta\text{-PH-GFP}$ from the cytosolic face of the membrane in cells infected by wild-type, but not SigD-deficient, *Salmonella*. More recently, the appearance of $\text{PtdIns}(3)\text{P}$ in *Salmonella*-containing vacuoles was also attributed to the lipid phosphatase activity of SigD (Hernandez et al., 2004). Here we provide direct biochemical evidence of phosphoinositide conversion induced by SigD. Cells infected by *Salmonella* were found to have a markedly elevated content of 4' and/or 5'-phosphorylated PtdInsP , which corresponded quantitatively to the concomitant decrease in $\text{PtdIns}(4,5)\text{P}_2$.

At least a fraction of the product was $\text{PtdIns}(5)\text{P}$, a lipid that is expressed in minute amounts in untreated cells. The increase in $\text{PtdIns}(5)\text{P}$ induced by SigD is strongly reminiscent of the effect of IpgD, a *Shigella* virulence factor that bears considerable sequence homology (38.5%) with SigD. IpgD concomitantly produced depletion of $\text{PtdIns}(4,5)\text{P}_2$, pointing to dephosphorylation of this inositide at the 4' position as the source of $\text{PtdIns}(5)\text{P}$. Indeed, like SigD, IpgD bears a region of homology with mammalian inositol 4-phosphatases (Norris et al., 1998). Thus, both the *Shigella* and *Salmonella* phosphatases appear to target primarily $\text{PtdIns}(4,5)\text{P}_2$ and, as such, are very useful tools to study the functional requirement for this phosphoinositide in animal cells.

Tools for the Manipulation of $\text{PtdIns}(4,5)\text{P}_2$ in Intact Mammalian Cells

While phospholipids were initially thought to serve mainly a structural role, they are now believed to participate in signaling, vesicular traffic, and cytoskeleton regulation. Some of these suggested functions have been deduced from in vitro experiments but require verification in intact cells. Such verification has been most difficult, largely because selective manipulation of specific inositides has proven extremely complex. In the case of $\text{PtdIns}(4,5)\text{P}_2$, several strategies have been attempted. Metabolic inhibition has been found to be paralleled by depletion of $\text{PtdIns}(4,5)\text{P}_2$. However, the specificity of this manipulation is questionable, in view of the myriad ATP-dependent events in cells. $\text{PtdIns}(4,5)\text{P}_2$ is often depleted acutely by activation of phospholipase C using calcium ionophores (Varnai and Balla, 1998). As in the case of ATP depletion, however, the pleiotropic effects of calcium elevation make assignment of functional consequences ambiguous. More specific effects can, in principle, be obtained using phosphoinositide-specific phosphatases. Several 5-phosphatases have been identified and reported to cleave $\text{PtdIns}(4,5)\text{P}_2$. We have tested heterologous overexpression of OCRL and SKIP, with negligible effects on $\text{PtdIns}(4,5)\text{P}_2$ content

(unpublished data). This may be attributed to the subcellular location of these enzymes, which are found mostly in endomembranes (Gurung et al., 2003; Ungewickell et al., 2004). In our hands, heterologous expression of Inp54p, a 5-phosphatase from yeast, had only minor effects on epithelial cells. We were similarly disappointed by the effects of overexpressed full-length synaptojanin (unpublished data), even though this phosphatase is found at the plasma membrane (McPherson et al., 1996). It is conceivable that synaptojanin, and possibly the other 5-phosphatases as well, require the coexpression of ancillary factors and/or are regulated by heretofore unidentified mechanisms.

A constitutively active phosphatase that does not require cofactors and is not subject to regulation would be more suitable to acutely manipulate PtdIns(4,5)P₂. Our observations suggest that bacterial 4-phosphatases, such as SigD and IpgD, fulfill these requirements and have ample activity to induce massive degradation of PtdIns(4,5)P₂ in a variety of mammalian cells. These enzymes can be expressed heterologously in eukaryotic cells by introduction of the available cDNAs, and recombinant proteins could in principle be used for microinjection when even more acute effects are desired. Unlike the synaptojanin-CAAX construct, the bacterial phosphatases do not require posttranslational modifications, which facilitates recombinant expression and accelerates generation of the active protein in transfected cells. It must be borne in mind that both SigD and IpgD generate PtdIns(5)P in the plasmalemma as they degrade PtdIns(4,5)P₂ and that this product may have biological activity, although none has been described to date and we failed to observe any effects following intracellular delivery of PtdIns(5)P. Nevertheless, a bioactive role for PtdIns(5)P cannot be ruled out.

Effects of PtdIns(4,5)P₂ Depletion on Epithelial Structure and Function

Expression of SigD was accompanied by marked changes in the structure of epithelial cells. These were likely caused by the depletion of plasmalemmal PtdIns(4,5)P₂, since neither PtdIns(5)P nor IP₄, the known products of SigD activity, were able to recapitulate the structural changes. Evidence that PtdIns(4,5)P₂ depletion can alter the actin cytoskeleton was provided by Raucher et al. (2000), who used optical tweezers to measure membrane tether forces in nonpolarized cells expressing Inp54p, a 5-phosphatase from yeast. Our results expressing synaptojanin-CAAX and 2(PLCδ-PH)-GFP are also consistent with a requirement for normal levels of PtdIns(4,5)P₂ to maintain intact the epithelial structure.

The effects of PtdIns(4,5)P₂ depletion on cytoskeletal architecture followed a peculiar time course. At the earliest stages, the cells emitted apical lamellipodial extensions, and this coincided with extensive vacuolation. Subsequently, stress fibers disappeared gradually as the

overall F-actin content diminished and the cells ultimately underwent blebbing and rounding as they protruded from the monolayer. Inactivation of ezrin likely contributed to disruption of the apical structure, since this protein is thought to anchor transmembrane proteins to actin fibers in a manner that is stimulated by PtdIns(4,5)P₂ (Bretscher et al., 2002). The perijunctional actin band was also depleted upon hydrolysis of PtdIns(4,5)P₂ and this was associated with loss of ZO-1 staining, consistent with junctional uncoupling. The loss of cell-cell contacts can readily explain the extrusion of the SigD-transfected cells from the context of the epithelial monolayer. To our knowledge, this is the first evidence that tight junctional integrity depends on the availability of PtdIns(4,5)P₂.

We also assessed the consequences of PtdIns(4,5)P₂ depletion on a limited number of physiological parameters characteristic of epithelia. First, we noted that Na⁺/H⁺ exchange was severely depressed by reducing the level of the phosphoinositide. These observations are in good agreement with earlier reports in non-epithelial model systems (Aharonovitz et al., 2000; Fuster et al., 2004) and emphasize the multiplicity of actions of PtdIns(4,5)P₂. It remains unclear whether the effects of the phospholipid are exerted directly or via intermediate proteins like ezrin (Baumgartner et al., 2004). In any event, it is clear that conditions predicted to alter PtdIns(4,5)P₂, such as ischemia or infection by *Salmonella* or *Shigella*, will be accompanied by reduced salt and water absorption and may thus contribute to overall fluid loss during diarrhea (see below).

Contribution of PtdIns(4,5)P₂ Loss to Diarrhea Induced by Pathogenic Bacteria

The occurrence of diarrhea is one of the major clinical complications of infection by *Salmonella*. Targeted deletion experiments initially demonstrated that the bacterial factors responsible for the fluid loss resided in the first pathogenicity island of the *Salmonella* genome (SPI 1). Further refinements of the deletional analysis indicated that the effector proteins SipA, SopA, SigD/SopB, SopD, and SopE2 act in concert to induce diarrhea (Zhang et al., 2002). The individual contribution of each of these proteins has not been thoroughly defined, but SigD is believed to be a major effector and has therefore been studied in most detail. In particular, it has been proposed that SigD contributes to fluid loss by stimulation of intestinal chloride secretion, and this effect was postulated to be mediated by IP₄ (Feng et al., 2001). The rationale for this proposal is based on the earlier report that PtdIns(3,4,5)P₃ acts as an inhibitor of calcium-dependent chloride secretion (Eckmann et al., 1997). By competing with PtdIns(3,4,5)P₃, IP₄ was proposed to relieve this inhibition, unmasking chloride secretion. In support of this hypothesis, Feng et al. (2001) reported that expression of SigD in HEK293

cells promoted an increase in chloride permeability. However, this hypothesis appears unlikely on the following grounds. (a) Chloride secretion is not constitutive and requires an increase in cytosolic calcium above the basal level. Indeed, the inhibitory effect of PtdIns(3,4,5)P₃ is exerted on the secretion induced by muscarinic agents, but is not expected to occur in otherwise unstimulated cells. (b) The purported inhibitory effect of IP₄ requires competition with existing PtdIns(3,4,5)P₃. However, the resting levels of apical PtdIns(3,4,5)P₃ in unstimulated cells are very low, insufficient to raise basal calcium by activation of phospholipase C γ (Melendez et al., 1999) or of Tec-family kinases, if present (Carpenter, 2004). (c) *Shigella*, which is related to *Salmonella* and produces a similar diarrhea, was reported by Eckmann et al. (1997) not to generate IP₄. (d) Lastly, the reported effects of SigD on chloride permeability appear not to be universal and, importantly, were not observed in intestinal epithelial cells in our experiments. Jointly, these considerations detract from the weight that should be given to IP₄ and chloride secretion as contributing factors to *Salmonella*-induced diarrhea.

The experiments presented here suggest alternative mechanisms. First, depletion of PtdIns(4,5)P₂ by SigD resulted in inhibition of Na⁺/H⁺ exchange activity, which is predicted to depress the rate of sodium and water absorption (by inhibition of NHE3) and compromise intracellular pH homeostasis (by inhibition of NHE1). At later stages, cells expressing SigD lost F-actin and underwent opening of their junctional complexes. The ensuing transient increase in transepithelial conductance could readily account for decreased fluid absorption. Indeed, junctional opening has been invoked in the etiology of diarrhea in both bacterial and viral infections (Dickman et al., 2000; Goosney et al., 2000; Bertelsen et al., 2004).

Clearly, though informative, microinjection of SigD into IEC-18 cells is not a perfect model of bacterial infection. This paradigm is useful in that it enabled us to isolate the contribution of SigD to the bacterial effector phenotype. On the other hand, neither the intensity nor the duration of the effects of expressed SigD are likely to be identical to those it exerts during bacterial infection. In the heterologous expression system SigD is likely to localize to both apical and basolateral membranes, which may not be the case during infection. Lastly, though derived from the rat ileum (Ma et al., 1992), IEC-18 cells are not perfect mimics of the primary epithelium. Nevertheless, the information obtained revealed the potential of SigD to exert a variety of biological effects, the contribution of which to the pathogenicity of the bacteria will need to be validated *in vivo*.

We thank Ms. Natasha Coady-Osberg and Mr. Michael Woodside for technical assistance and Drs. H. Tronchère and C. Pendaries for helpful discussions.

This work was supported by grants from the Canadian Institutes of Health Research (CIHR), the Association pour la Recherche sur le Cancer contract no. 4794, and ARECA-Toulouse. B.B. Finlay is a Distinguished Investigator of the CIHR and the UBC Peter Wall Distinguished Professor. J.H. Brumel holds an Investigator in Pathogenesis of Infectious Disease Award from the Burroughs Wellcome Fund. S. Grinstein is the current holder of the Pitblado Chair in Cell Biology.

Lawrence G. Palmer served as editor.

Submitted: 28 August 2006

Accepted: 2 March 2007

REFERENCES

- Aharonovitz, O., H.C. Zaun, T. Balla, J.D. York, J. Orlowski, and S. Grinstein. 2000. Intracellular pH regulation by Na⁺/H⁺ exchange requires phosphatidylinositol 4,5-bisphosphate. *J. Cell Biol.* 150:213–224.
- Baumgartner, M., H. Patel, and D.L. Barber. 2004. Na⁺/H⁺ exchanger NHE1 as plasma membrane scaffold in the assembly of signaling complexes. *Am. J. Physiol. Cell Physiol.* 287:C844–C850.
- Bertelsen, L.S., G. Paesold, S.L. Marcus, B.B. Finlay, L. Eckmann, and K.E. Barrett. 2004. Modulation of chloride secretory responses and barrier function of intestinal epithelial cells by the *Salmonella* effector protein SigD. *Am. J. Physiol. Cell Physiol.* 287:C939–C948.
- Botelho, R.J., M. Teruel, R. Dierckman, R. Anderson, A. Wells, J.D. York, T. Meyer, and S. Grinstein. 2000. Localized biphasic changes in phosphatidylinositol-4,5-bisphosphate at sites of phagocytosis. *J. Cell Biol.* 151:1353–1368.
- Bretscher, A., K. Edwards, and R.G. Fehon. 2002. ERM proteins and merlin: integrators at the cell cortex. *Nat. Rev. Mol. Cell Biol.* 3:586–599.
- Carpenter, C.L. 2004. Btk-dependent regulation of phosphoinositide synthesis. *Biochem. Soc. Trans.* 32:326–329.
- Carricaburu, V., K.A. Lamia, E. Lo, L. Favereaux, B. Payrastré, L.C. Cantley, and L.E. Rameh. 2003. The phosphatidylinositol (PI)-5-phosphate 4-kinase type II enzyme controls insulin signaling by regulating PI-3,4,5-triphosphate degradation. *Proc. Natl. Acad. Sci. USA.* 100:9867–9872.
- Counillon, L., W. Scholz, H.J. Lang, and J. Pouyssegur. 1993. Pharmacological characterization of stably transfected Na⁺/H⁺ antiporter isoforms using amiloride analogs and a new inhibitor exhibiting anti-ischemic properties. *Mol. Pharmacol.* 44:1041–1045.
- Dickman, K.G., S.J. Hempson, J. Anderson, S. Lippe, L. Zhao, R. Burakoff, and R.D. Shaw. 2000. Rotavirus alters paracellular permeability and energy metabolism in Caco-2 cells. *Am. J. Physiol. Gastrointest. Liver Physiol.* 279:G757–G766.
- Djordjevic, S., and P.C. Driscoll. 2002. Structural insight into substrate specificity and regulatory mechanisms of phosphoinositide 3-kinases. *Trends Biochem. Sci.* 27:426–432.
- Eckmann, L., M.T. Rudolf, A. Ptasznik, C. Schultz, T. Jiang, N. Wolfson, R. Tsien, J. Fierer, S.B. Shears, M.F. Kagnoff, and A.E. Traynor-Kaplan. 1997. D-myo-inositol 1,4,5,6-tetrakisphosphate produced in human intestinal epithelial cells in response to *Salmonella* invasion inhibits phosphoinositide 3-kinase signaling pathways. *Proc. Natl. Acad. Sci. USA.* 94:14456–14460.
- Estacion, M., W.G. Sinkins, and W.P. Schilling. 2001. Regulation of *Drosophila* transient receptor potential-like (TrpL) channels by phospholipase C-dependent mechanisms. *J. Physiol.* 530:1–19.
- Feng, Y., S.R. Wenthe, and P.W. Majerus. 2001. Overexpression of the inositol phosphatase SopB in human 293 cells stimulates cellular chloride influx and inhibits nuclear mRNA export. *Proc. Natl. Acad. Sci. USA.* 98:875–879.

- Fuster, D., O.W. Moe, and D.W. Hilgemann. 2004. Lipid- and mechanosensitivities of sodium/hydrogen exchangers analyzed by electrical methods. *Proc. Natl. Acad. Sci. USA*. 101:10482–10487.
- Galan, J.E. 1998. Interactions of *Salmonella* with host cells: encounters of the closest kind. *Proc. Natl. Acad. Sci. USA*. 95:14006–14008.
- Galyov, E.E., M.W. Wood, R. Rosqvist, P.B. Mullan, P.R. Watson, S. Hedges, and T.S. Wallis. 1997. A secreted effector protein of *Salmonella dublin* is translocated into eukaryotic cells and mediates inflammation and fluid secretion in infected ileal mucosa. *Mol. Microbiol.* 25:903–912.
- Goosney, D.L., S. Gruenheid, and B.B. Finlay. 2000. Gut feelings: enteropathogenic *E. coli* (EPEC) interactions with the host. *Annu. Rev. Cell Dev. Biol.* 16:173–189.
- Gurung, R., A. Tan, L.M. Ooms, M.J. McGrath, R.D. Huysmans, A.D. Munday, M. Prescott, J.C. Whisstock, and C.A. Mitchell. 2003. Identification of a novel domain in two mammalian inositol-polyphosphate 5-phosphatases that mediates membrane ruffle localization. The inositol 5-phosphatase skip localizes to the endoplasmic reticulum and translocates to membrane ruffles following epidermal growth factor stimulation. *J. Biol. Chem.* 278:11376–11385.
- Hernandez, L.D., K. Hueffer, M.R. Wenk, and J.E. Galan. 2004. *Salmonella* modulates vesicular traffic by altering phosphoinositide metabolism. *Science*. 304:1805–1807.
- Hilgemann, D.W., S. Feng, and C. Nasuhoglu. 2001. The complex and intriguing lives of PIP₂ with ion channels and transporters. *Sci. STKE*. 2001:re19.
- Hilgemann, D.W. 2003. Getting ready for the decade of the lipids. *Annu. Rev. Physiol.* 5:697–700.
- Hilpela, P., M.K. Vartiainen, and P. Lappalainen. 2004. Regulation of the actin cytoskeleton by PI(4,5)P₂ and PI(3,4,5)P₃. *Curr. Top. Microbiol. Immunol.* 282:117–163.
- Ho, H.Y., R. Rohatgi, A.M. Lebensohn, L. Ma, J. Li, S.P. Gygi, and M.W. Kirschner. 2004. Toca-1 mediates Cdc42-dependent actin nucleation by activating the N-WASP-WIP complex. *Cell*. 118:203–216.
- Jayaraman, S., P. Haggie, R.M. Wachter, S.J. Remington, and A.S. Verkman. 2000. Mechanism and cellular applications of a green fluorescent protein-based halide sensor. *J. Biol. Chem.* 275:6047–6050.
- Knodler, L.A., and B.B. Finlay. 2001. *Salmonella* and apoptosis: to live or let die? *Microbes Infect.* 3:1321–1326.
- Lemmon, M.A. 2003. Phosphoinositide recognition domains. *Traffic*. 4:201–213.
- Leung, Y.M., W.Z. Zeng, H.H. Liou, C.R. Solaro, and C.L. Huang. 2000. Phosphatidylinositol 4,5-bisphosphate and intracellular pH regulate the ROMK1 potassium channel via separate but inter-related mechanisms. *J. Biol. Chem.* 275:10182–10189.
- Loussouarn, G., K.H. Park, C. Bellocq, I. Baro, F. Charpentier, and D. Escande. 2003. Phosphatidylinositol-4,5-bisphosphate, PIP₂, controls KCNQ1/KCNE1 voltage-gated potassium channels: a functional homology between voltage-gated and inward rectifier K⁺ channels. *EMBO J.* 22:5412–5421.
- Ma, T.Y., D. Hollander, D. Bhalla, H. Nguyen, and P. Krugliak. 1992. IEC-18, a nontransformed small intestinal cell line for studying epithelial permeability. *J. Lab. Clin. Med.* 120:329–341.
- Majno, G., and J. Joris. 1995. Apoptosis, oncosis, and necrosis. An overview of cell death. *Am. J. Pathol.* 146:3–15.
- Malecz, N., P.C. McCabe, C. Spaargaren, R. Qiu, Y. Chuang, and M. Symons. 2000. Synaptojanin 2, a novel Rac1 effector that regulates clathrin-mediated endocytosis. *Curr. Biol.* 10:1383–1386.
- Marcus, S.L., M.R. Wenk, O. Steele-Mortimer, and B.B. Finlay. 2001. A synaptojanin-homologous region of *Salmonella typhimurium* SigD is essential for inositol phosphatase activity and Akt activation. *FEBS Lett.* 494:201–207.
- Marcus, S.L., L.A. Knodler, and B.B. Finlay. 2002. *Salmonella enterica* serovar Typhimurium effector SigD/SopB is membrane-associated and ubiquitinated inside host cells. *Cell. Microbiol.* 4:435–446.
- Matsui, S., R. Adachi, K. Kusui, T. Yamaguchi, T. Kasahara, T. Hayakawa, and K. Suzuki. 2001. U73122 inhibits the dephosphorylation and translocation of cofilin in activated macrophage-like U937 cells. *Cell. Signal.* 13:17–22.
- McPherson, P.S., E.P. Garcia, V.I. Slepnev, C. David, X. Zhang, D. Grabs, W.S. Sossin, R. Bauerfeind, Y. Nemoto, and P. De Camilli. 1996. A presynaptic inositol-5-phosphatase. *Nature*. 379:353–357.
- Melendez, A.J., M.M. Harnett, and J.M. Allen. 1999. FcγRI activation of phospholipase Cγ1 and protein kinase C in dibutyryl cAMP-differentiated U937 cells is dependent solely on the tyrosine-kinase activated form of phosphatidylinositol-3-kinase. *Immunology*. 98:1–13.
- Morris, J.B., K.A. Hinchliffe, A. Ciruela, A.J. Letcher, and R.F. Irvine. 2000. Thrombin stimulation of platelets causes an increase in phosphatidylinositol 5-phosphate revealed by mass assay. *FEBS Lett.* 475:57–60.
- Nebl, T., S.W. Oh, and E.J. Luna. 2000. Membrane cytoskeleton: PIP(2) pulls the strings. *Curr. Biol.* 10:R351–R354.
- Niebuhr, K., S. Giuriato, T. Pedron, D.J. Philpott, F. Gaits, J. Sable, M.P. Sheetz, C. Parsot, P.J. Sansonetti, and B. Payrastre. 2002. Conversion of PtdIns(4,5)P(2) into PtdIns(5)P by the *S. flexneri* effector IpgD reorganizes host cell morphology. *EMBO J.* 21:5069–5078.
- Norris, F.A., M.P. Wilson, T.S. Wallis, E.E. Galyov, and P.W. Majerus. 1998. SopB, a protein required for virulence of *Salmonella dublin*, is an inositol phosphate phosphatase. *Proc. Natl. Acad. Sci. USA*. 95:14057–14059.
- Oliver, D., C.C. Lien, M. Soom, T. Baukowitz, P. Jonas, and B. Fakler. 2004. Functional conversion between A-type and delayed rectifier K⁺ channels by membrane lipids. *Science*. 304:265–270.
- Raucher, D., T. Stauffer, W. Chen, K. Shen, S. Guo, J.D. York, M.P. Sheetz, and T. Meyer. 2000. Phosphatidylinositol 4,5-bisphosphate functions as a second messenger that regulates cytoskeleton-plasma membrane adhesion. *Cell*. 100:221–228.
- Roth, M.G. 2004. Phosphoinositides in constitutive membrane traffic. *Physiol. Rev.* 84:699–730.
- Santos, R.L., R.M. Tsois, S. Zhang, T.A. Ficht, A.J. Baumler, and L.G. Adams. 2001. *Salmonella*-induced cell death is not required for enteritis in calves. *Infect. Immun.* 69:4610–4617.
- Serunian, L.A., K.R. Auger, and L.C. Cantley. 1991. Identification and quantification of polyphosphoinositides produced in response to platelet-derived growth factor stimulation. *Methods Enzymol.* 198:78–87.
- Spitaler, M., and D.A. Cantrell. 2004. Protein kinase C and beyond. *Nat. Immunol.* 5:785–790.
- Stauffer, T.P., S. Ahn, and T. Meyer. 1998. Receptor-induced transient reduction in plasma membrane PtdIns(4,5)P₂ concentration monitored in living cells. *Curr. Biol.* 8:343–346.
- Taylor, C.W. 2002. Controlling calcium entry. *Cell*. 111:767–769.
- Terebiznik, M.R., O.V. Vieira, S.L. Marcus, A. Slade, C.M. Yip, W.S. Trimble, T. Meyer, B.B. Finlay, and S. Grinstein. 2002. Elimination of host cell PtdIns(4,5)P(2) by bacterial SigD promotes membrane fission during invasion by *Salmonella*. *Nat. Cell Biol.* 4:766–773.
- Teruel, M.N., T.A. Blanpied, K. Shen, G.J. Augustine, and T. Meyer. 1999. A versatile microinjection technique for the transfection of cultured CNS neurons. *J. Neurosci. Methods*. 93:37–48.
- Tronchere, H., J. Laporte, C. Pendaries, C. Chaussade, L. Liaubet, L. Pirola, J.L. Mandel, and B. Payrastre. 2004. Production of phosphatidylinositol 5-phosphate by the phosphoinositide 3-phosphatase myotubularin in mammalian cells. *J. Biol. Chem.* 279:7304–7312.

- Ungewickell, A., M.E. Ward, E. Ungewickell, and P.W. Majerus. 2004. The inositol polyphosphate 5-phosphatase Ocr1 associates with endosomes that are partially coated with clathrin. *Proc. Natl. Acad. Sci. USA.* 101:13501–13506.
- Uzzau, S., and A. Fasano. 2000. Cross-talk between enteric pathogens and the intestine. *Cell. Microbiol.* 2:83–89.
- Vanhaesebroeck, B., S.J. Leever, K. Ahmadi, J. Timms, R. Katso, P.C. Driscoll, R. Woscholski, P.J. Parker, and M.D. Waterfield. 2001. Synthesis and function of 3-phosphorylated inositol lipids. *Annu. Rev. Biochem.* 70:535–602.
- Varnai, P., and T. Balla. 1998. Visualization of phosphoinositides that bind pleckstrin homology domains: calcium- and agonist-induced dynamic changes and relationship to myo-[3H]inositol-labeled phosphoinositide pools. *J. Cell Biol.* 143:501–510.
- Varnai, P., X. Lin, S.B. Lee, G. Tuymetova, T. Bondeva, A. Spat, S.G. Rhee, G. Hajnoczky, and T. Balla. 2002. Inositol lipid binding and membrane localization of isolated pleckstrin homology (PH) domains. Studies on the PH domains of phospholipase C delta 1 and p130. *J. Biol. Chem.* 277:27412–27422.
- Verkman, A.S., M.C. Sellers, A.C. Chao, T. Leung, and R. Ketcham. 1989. Synthesis and characterization of improved chloride-sensitive fluorescent indicators for biological applications. *Anal. Biochem.* 178:355–361.
- Vieira, O.V., R.J. Botelho, L. Rameh, S.M. Brachmann, T. Matsuo, H.W. Davidson, A. Schreiber, J.M. Backer, L.C. Cantley, and S. Grinstein. 2001. Distinct roles of class I and class III phosphatidylinositol 3-kinases in phagosome formation and maturation. *J. Cell Biol.* 155:19–25.
- Zhang, S., R.L. Santos, R.M. Tsois, S. Stender, W.S. Hardt, A.J. Baumler, and L.G. Adams. 2002. The *Salmonella enterica* serotype typhimurium effector proteins SipA, SopA, SopB, SopD, and SopE2 act in concert to induce diarrhea in calves. *Infect. Immun.* 70:3843–3855.
- Zhou, D., L.M. Chen, L. Hernandez, S.B. Shears, and J.E. Galan. 2001. A *Salmonella* inositol polyphosphatase acts in conjunction with other bacterial effectors to promote host cell actin cytoskeleton rearrangements and bacterial internalization. *Mol. Microbiol.* 39:248–259.